SCIENCE CHINA
Earth Sciences

•RESEARCH PAPER•

December 2019 Vol.62 No.12: 2069–2082
https://doi.org/10.1007/s11430-018-9378-1

The macroscopic mechanisms and associated atmospheric precursor environmental capacities that lead to secondary fine particle pollution

Dahai XU* & Junming CHEN

State Key Laboratory of Severe Weather and Key Laboratory of Atmospheric Chemistry of China Meteorological Administration, Chinese Academy of Meteorological Sciences, Beijing 100081, China

Received August 3, 2018; revised May 15, 2019; accepted June 11, 2019; published online September 5, 2019

Abstract This paper establishes the kinetic equations in atmospheric chemistry that describe the macroscopic mechanisms of secondary fine particle pollution generated by precursors during atmospheric self-purification. The dynamic and static solutions of these equations can be applied to calculate quantitative relationships between the concentration ratio of precursors and secondary fine particles as well as the physical clearance power of the atmosphere, chemical reaction rate, and the scale of a contaminated area. The dynamic solution presented here therefore corresponds with a theoretical formula for calculating the overall rate constant for the oxidation reaction of reducing pollutants in the actual atmosphere based on their local concentrations and meteorological monitoring data. In addition, the static solution presented in this paper reveals the functional relationship between the concentration of secondary fine particles and precursor emission rate as well as atmospheric self-purification capacity. This result can be applied to determine the atmospheric environmental capacity of a precursor. Hourly records collected over the last 40 years from 378 weather stations in mainland China as well as the spatiotemporal distribution sequence of overall oxidation reaction rates from precursors show that when the reference concentration limit of secondary fine particles is 100 μmol m^{-3}, the atmospheric environmental capacity of total precursors can be calculated as 24890×10^{10} mol yr^{-1}. Thus, when the annual average concentration limit of given fine particles is 35 μg m^{-3} and the ratio of sulfate and nitrate to 30% and 20% of the total amount of fine particles, the capacities of SO_2, NO_x and NH_3 are 1255, 1344, and 832 (10^{10}g yr^{-1}), respectively. The clearance density of precursors for different return periods across mainland China under above conditions are also provided in this study.

Keywords Atmospheric chemical kinetic equations, Precursor of secondary fine particle, Overall oxidation reaction rate, Atmospheric self-purification power, Atmospheric environmental capacity, Clearance density, Return period

Citation: Xu D, Chen J. 2019. The macroscopic mechanisms and associated atmospheric precursor environmental capacities that lead to secondary fine particle pollution. Science China Earth Sciences, 62: 2069–2082, https://doi.org/10.1007/s11430-018-9378-1

1. Introduction

Fine particles, $PM_{2.5}$, are major air pollutants and include sulfates, nitrates, organic and inorganic carbon, as well as various other oxides (Zhou et al., 2017; Jiang et al., 2017; Xing et al., 2016; Gu et al., 2016; Deng et al., 2011; Xu et al., 2017; Zhang et al., 2011; Wei et al., 2017; Lin et al., 2017; Cao et al., 2014). These fine particles mainly originate from reducing primary contaminants in the atmosphere, including the products of SO_2, NO_x and hydrocarbon RH oxidation reactions (referred to here as precursors). A number of studies have induced and summarized oxidation rates from various reducing substances and corresponding oxidants for the processes controlling these types of precursors (Tang et

* Corresponding author (email: xudh2013@qq.com)

al., 2006; Cheng et al., 2008; Seinfeld and Pandis, 2016; Li et al., 2017), leading to the generation of numerous effective air quality models (Grell et al., 2005; Byun and Schere, 2006). On this basis, a number of atmospheric environmental science researches and environmental air management projects have been performed using these simulation tools and corresponding inventories. In order to confirm the basis of these source lists, however, clearly defined resolution tools (Cooper and Watson, 1980; Paatero and Tapper, 1993) are required. It therefore remains difficult to determine the limits of specific precursor emissions based on their management, secondary fine particles at the macroscopic level, and the concentration of fine particles because of the nature of statistical time lags and source lists as well as variabilities in meteorological conditions and the multiplicity of inherent problems.

Temporal variations in atmospheric pollutant concentrations are caused by balancing between emission and the natural clearance of pollutants. Natural clearance in the atmosphere is mainly determined by chemical oxidation and physical clearance powers, which are formed by advective ventilation, turbulent diffusion, and dry and wet settling. Although Xu et al. (2016, 2018) investigated the role of physical clearance power in the formation of atmospheric environmental capacity, no quantitative analysis that incorporates atmospheric oxidation processes has so far been performed. However, unlike physical clearance power, chemical clearance power is a sink of reducing species in the atmosphere pollutants as well as a source of secondary pollutants formed after oxidation, which changes the composition of these elements in the atmosphere. The atmospheric chemical clearance power of certain reducing species can usually be represented by the oxidation rate of a corresponding agent. At the same time, the precursors of fine particles emitted into atmosphere by natural processes and human activities are not single species and oxidants involved in these reactions are complex. The most important include OH radicals as well as total oxidants, O_x (roughly equivalent to O_3+NO_2), peroxide radicals (HO_2 and RO_2), peroxides (H_2O_2 and ROOH), NO_3 radicals, and halogen radicals. Specifically, OH plays a key role in chemical processes that occur during daylight hours, while NO_3, N_2O_5, and O_3 are active at night. It is also very difficult to accurately detect the spatiotemporal variation in these oxidants separately in the atmosphere because they are highly chemical reactive, low in concentration, and have a short lifespan. The literature (Cheng et al., 2008) points out the above facts, and treats overall reducing pollutants in the atmosphere as a type of lumped precursor, and the corresponding oxidation products as lumped secondary pollutants, and the oxidation of the above lumped precursors is considered to be carried out in a pseudo first order process. They use atmospheric pollution numerical simulation to determine $k_{\mathrm{por},T}$ the overall rate of the pseudo-first-order oxidation reaction (indicated simply by K in this paper) to replace the actual monitoring. This method essentially adopts the concept of a lumped mechanism (Tang et al., 2006) which makes the most generalized induction regarding the oxidation processes of reducing pollutants in the atmosphere. Thus, based on this concept and using physical self-purification force and chemical clearance power represented by K as driving forces, atmospheric chemical kinetic equations that describe changes in precursor concentrations and oxidation products were established in this study.

The emission of precursors, formation of secondary products, and evolutionary mechanisms under the action of atmospheric physical clearance power were analyzed here based on equation solutions, while the regional atmospheric environmental capacity of secondary fine particle pollutant precursors were also estimated. As the chemical process discussed in this study is an oxidation reaction, its secondary consequences can also be referred to as oxidation products. Indeed, whether, or not, an oxidation product is a fine particle depends on a reducing contaminant species, oxidizing agents, and concerned specific products.

The definition of atmospheric environmental capacity used here follows that defined by Xu et al. (2013, 2016). In other words, for a given volume in atmosphere and time interval, when pollutant generation (source) and removal (sink) reach a balance, the pollutant concentration maintains a specified value (threshold concentration), and the rate of pollutant generation (emission) is defined as the atmospheric environmental capacity under the threshold concentration.

2. Methods

2.1 Atmospheric chemical kinetic equations

In order to discuss the quantitative effects of physical processes and oxidation processes on the self-purification of the atmosphere, it is first essential to establish an appropriate Kinetic equation.

Based on the literature (Cheng et al., 2008), a Kinetic equation that expresses the pseudo-first-order oxidation reaction for removing the reducing substances c_i i=1,⋯, n from the atmosphere is as follows:

$$c_i + x_j = p_{i,j},\ k_{i,j},\ j=1,\cdots,m. \tag{1}$$

In this expression, x_j is the oxidant j in the reaction, $p_{i,j}$ denotes the oxidation product of the reductive substance i by oxidant j, and $k_{i,j}$ is the reaction rate constant of the corresponding pseudo-first-order oxidation. The resultant equations for calculating the change in c_i molar concentration is therefore:

$$\frac{\mathrm{d}}{\mathrm{d}t}[c_i] = -K_i[c_i]. \tag{2}$$

Similarly, the formula for calculating the change in total molar concentration of all j oxidation products $[p_i] = \sum_{j=1}^{m}[p_{i,j}]$ corresponding to c_i over time t is as follows:

$$\frac{\mathrm{d}}{\mathrm{d}t}[p_i]=K_i[c_i], \tag{3}$$

thus:

$$K_i=\sum_{j=1}^{m} k_{i,j}[x_j]. \tag{4}$$

Assuming $[C] = \sum_{i=1}^{n}[c_i]$, $[P] = \sum_{i=1}^{n}[p_i]$, eqs. (2) and (3) can be expressed as:

$$\frac{\mathrm{d}}{\mathrm{d}t}[C] = -K[C], \tag{5}$$

$$\frac{\mathrm{d}}{\mathrm{d}t}[P] = K[C]. \tag{6}$$

In these expressions, K denotes the overall oxidation reaction rate as defined by Cheng et al. (2008), and therefore:

$$K = \sum_{i=1}^{n}\sum_{j=1}^{m} k_{i,j}[x_j][c_i] \ / \sum_{i=1}^{n}[c_i]. \tag{7}$$

The individual derivative terms of eqs. (5) and (6) were then decomposed into local derivative and advective terms as well as the source, diffusion, and settlement of pollutants were introduced.

Concentration $[C]$ was then replaced by the variable C for convenience and $[P]$ was replaced by P to constitute a pair of basic equations for atmospheric chemical kinetic equations, as follows:

$$\frac{\partial C}{\partial t} + \mathbf{V}\cdot\nabla C = \sum_l q_{cl}\delta(\mathbf{r}_l) - (\mathbf{v}_d+\mathbf{v}_w)_c \cdot\nabla C - KC + \nabla\cdot\boldsymbol{\mathcal{K}}\cdot\nabla C, \tag{8}$$

$$\frac{\partial P}{\partial t} + \mathbf{V}\cdot\nabla P = \sum_l q_{pl}\delta(\mathbf{r}_l) - (\mathbf{v}_d+\mathbf{v}_w)_p \cdot\nabla P + KC + \nabla\cdot\boldsymbol{\mathcal{K}}\cdot\nabla P. \tag{9}$$

In these expressions, C and P denote the molar concentrations of reductant and oxidation products, respectively, while $\mathbf{V}$ denotes advection velocity, q_{cl} and q_{pl} refer to the molar intensity of the source (sink) of reducing substances and oxidation products at position $\mathbf{r}_l$, respectively, $\delta(\mathbf{r}_l)$ is the Dirac Delta function, $\boldsymbol{\mathcal{K}}$ is the tensor of turbulent exchange coefficient, $(\mathbf{v}_d+\mathbf{v}_w)_c$ and $(\mathbf{v}_d+\mathbf{v}_w)_p$ refer to the dry and wet settling velocity vectors of reducing substances and oxidation products, respectively. The three-components of these latter two variables in space (x, y, z) are defined as follows:

$$(\mathbf{v}_d+\mathbf{v}_w)_{c,p} = \begin{cases} 0,0,0 & z\neq 0 \\ 0,0,(v_d+v_w)_{c,p} & z\to 0 \end{cases}.$$

This calculation also assumes that:

$$(\mathbf{v}_d+\mathbf{v}_w)_c \approx (\mathbf{v}_d+\mathbf{v}_w)_p = \mathbf{v}_d+\mathbf{v}_w.$$

Applying the method proposed by Xu and Zhu (2000) in tandem with the pseudo diffusion velocity $\mathbf{V}_t$ defined by Pasquill and Smith (1983), expressed as follows:

$$\mathbf{V}_t = -\frac{\boldsymbol{\mathcal{K}}\cdot\nabla C}{C} \approx -\frac{\boldsymbol{\mathcal{K}}\cdot\nabla P}{P}.$$

Thus, if eqs. (8) and (9) are integrated using the volume $\tau = HS$, the average concentration of reducing substances will be $\overline{C}$, and the average concentration of the oxidation product will be $\overline{P}$. It therefore follows that:

$$\overline{C} = \frac{1}{\tau}\iiint_\tau C\ \mathrm{d}\tau, \overline{P} = \frac{1}{\tau}\iiint_\tau P\ \mathrm{d}\tau.$$

According to the nature of the Dirac Delta function:

$$\iiint_\tau \sum_l q_{cl}\delta(\mathbf{r}_l)\ \mathrm{d}\tau = \sum_l q_{cl} = Q_c,$$

$$\iiint_\tau \sum_l q_{pl}\delta(\mathbf{r}_l)\ \mathrm{d}\tau = \sum_l q_{pl} = Q_p.$$

It therefore follows that Q_c and Q_p denote the primary emission rates of reducing substances and corresponding generated substances in volume τ, respectively.

Converting the volume integral to a surface integral, the following equations are generated:

$$\tau\frac{\partial\overline{C}}{\partial t} = Q_C - F_c\overline{C} - \tau K\overline{C}, \tag{10}$$

$$\tau\frac{\partial\overline{P}}{\partial t} = Q_P - F_p\overline{P} + \tau K\overline{C}. \tag{11}$$

The flux terms in these expressions are as follows:

$$F_c = \frac{1}{\overline{C}}\oiint_S C\left[\mathbf{V}+\mathbf{V}_t+(\mathbf{v}_d+\mathbf{v}_w)_c\right]\cdot\mathbf{ds}, \tag{12}$$

$$F_p = \frac{1}{\overline{P}}\oiint_S P\left[\mathbf{V}+\mathbf{V}_t+(\mathbf{v}_d+\mathbf{v}_w)_p\right]\cdot\mathbf{ds}, \tag{13}$$

and assumes that: $F_c \approx F_p = F$.

Eqs. (10) and (11) are atmospheric chemical kinetic equations that express the relationship between the emission of precursors and their oxidation products in the atmosphere, atmospheric physical removal, as well as the equilibrium between chemical sources and sinks. The clearing velocity vector is formed by combining ventilation, diffusion, and settlement within the surface integral, while the total pollutant flux at the boundary where the vector is generated is physical clearance power.

Chemical oxidation clearance power is expressed as the term of the overall rate, K, of the reaction. This set of equations can also be applied to the kinematic process of specific precursors and their oxidized products in the atmosphere; thus, K should represent the reaction rate of particular reducing substances and oxidants. This rate may also be related to physical self-purification capacity and so it is assumed that K and F are independent within the integration range in order to simplify this problem.

Throughout the integration of eqs. (12) or (13), it is assumed that the area of the integral curved surface on the ground is S. This variable, S, is sometimes referred to as the

area of the atmospheric pollutant reaction zone (short for reaction zone), while the side is a cylinder surface, the height, H, is that of the atmospheric boundary layer, volume is $\tau = HS$, concentration of pollutants entering the curved surface is zero, the concentration of pollutants flowing out of the curved surface is $\overline{C}$ or $\overline{P}$, and the advection-diffusion velocity of along the normal direction is U. It therefore follows that:

$$F = A\sqrt{S}. \tag{14}$$

In this expression, A is the atmospheric capacity coefficient defined in the Chinese National Standard (GB/T3840-91) as well as the atmospheric (physical) self-purification capability index defined in GB/T34299-2017. This is an important parameter in the air pollution potential index, as discussed by Zhu et al. (2018) and calculated as follows:

$$\begin{aligned} A &= \frac{\sqrt{\pi}UH}{2} + (v_d + v_w)\sqrt{S}, \\ U &= |\mathbf{V} + \mathbf{V}_t|_n . \end{aligned} \tag{15}$$

It follows that A comprises both ventilation and settlement terms. Across a general area or at the city scale, ventilation impact is much greater than that of sedimentation. It is also noteworthy that only the boundary advection-diffusion velocity along the normal direction acts on the ventilation, based on eqs. (12) and (13).

Throughout one integration period, if F, K, Q_c, and Q_p are constant, then eqs. (10) and (11) can be expressed as follows:

$$\frac{\partial \overline{C}}{\partial t} = \frac{Q_c}{HS} - \left(\frac{A}{H\sqrt{S}} + K\right)\overline{C}, \tag{16}$$

$$\frac{\partial \overline{P}}{\partial t} = \frac{Q_p}{HS} - \frac{A}{H\sqrt{S}}\overline{P} + K\overline{C}. \tag{17}$$

Eqs. (16) and (17) denote the local evolution of the concentration of reducing substances of precursors and their oxidation products, respectively, under the control of physical and chemical self-purification parameters.

2.2 Variations in precursor concentration: A solution to kinetic eq. (16)

It is clear that under equilibrium conditions, $\frac{\partial \overline{C}}{\partial t} = 0$, the solution $\overline{C}_\infty$ of eq. (16) is:

$$\overline{C}_\infty = \frac{Q_c}{A\sqrt{S} + HSK}, \tag{18}$$

$$Q_c = \overline{C}_\infty A\sqrt{S}\left(1 + \frac{H\sqrt{S}}{A}K\right). \tag{19}$$

Thus, under dynamic conditions, we assume $\overline{C} = \overline{C}_0$ when t=0, and therefore the solution of eq. (16) is:

$$\overline{C} - \overline{C}_\infty = (\overline{C}_0 - \overline{C}_\infty)\mathrm{e}^{-\left(\frac{A}{H\sqrt{S}}+K\right)t}. \tag{20}$$

Thus, according to Xu et al. (2018), it follows that:

$$\frac{A}{H\sqrt{S}} = \frac{1}{T_{ph}} = \frac{1}{T_L} + \frac{1}{T_h}, \tag{21}$$

where:

$$\begin{aligned} T_L &= L/U, \\ T_h &= H/(v_d + v_w), \\ L &= 2\sqrt{S/\pi}. \end{aligned} \tag{22}$$

In this expression, L denotes characteristic length scale, the equivalent diameter of area, S, while T_L is the time scale crossing dimension L of the zone under the advection- diffusion velocity U, T_h is average time taken to cross the thickness of the boundary layer under both dry and wet settling rates, and T_L and T_h constitute the characteristic time T_{ph} of physical existence of the pollutant in zone S. The larger the volume of this zone, the longer the characteristic physical existence time. Thus, if T_{ch} is set as the chemical lifetime of reductive pollutants, $T_{ch} = 1/K$, then the attenuation index in eq. (20) can be expressed as:

$$\frac{A}{H\sqrt{S}} + K = \frac{1}{T} = \frac{1}{T_{ph}} + \frac{1}{T_{ch}} = \frac{1}{T_L} + \frac{1}{T_h} + \frac{1}{T_{ch}}. \tag{23}$$

In other words, T denotes the comprehensive lifetime of a precursor and eq. (20) is

$$\overline{C} - \overline{C}_\infty = (\overline{C}_0 - \overline{C}_\infty)\mathrm{e}^{-\left(\frac{t}{T}\right)}. \tag{24}$$

On the basis of eq. (18), as weather conditions A and H change, a corresponding equilibrium concentration, $\overline{C}_\infty$, will be achieved while a certain time interval is required to reach this level. Thus, on the basis of eq. (24), time interval depends on comprehensive lifetime T, the value of which is mainly determined by the lower physical and chemical lifetimes. Physical lifetime in large areas, or cities, during static and small wind periods is long while chemical lifetime is relatively short, so the chemical processes are dominant. In the presence of strong winds, the physical lifetime of precursors will be much shorter than chemical lifetime and the clearance process of the former will be dominant.

Also, on the basis of eq. (20), it follows that:

$$K = \frac{\mathrm{Ln}\left[(\overline{C}_0 - \overline{C}_\infty)/(\overline{C} - \overline{C}_\infty)\right]}{t} - \frac{A}{H\sqrt{S}}. \tag{25}$$

According to the definition of physical residence period, T_{ph}, it follows that:

$$K = \frac{\mathrm{Ln}\left[(\overline{C}_0 - \overline{C}_\infty)/(\overline{C} - \overline{C}_\infty)\right]}{t} - \frac{1}{T_{ph}}. \tag{26}$$

Solutions to eqs. (25) or (26) provide an Euler method for determining the chemical reaction rate, K, based on monitored concentrations and characteristic physical existence times for reductive substances. This approach is more convenient than the classical Lagrange method that is used to track smog plume monitoring (Alkezweeny and Powell, 1977; State Environmental Protection Administration, 1991)

when applied to meteorological and concentration data in fixed-point monitoring programs. In the case of inactive substances, $K \approx 0$, eq. (26) suggests that:

$$T_{ph} = t / \mathrm{Ln}[(\overline{C}_0 - \overline{C}_\infty) / (\overline{C} - \overline{C}_\infty)]. \quad (27)$$

It is therefore theoretically feasible to obtain T_{ph} using eq. (27) based on time-varying data for the concentrations of inactive pollutant discharged in real time.

Once physical and chemical lifetimes have been defined based on eq. (21), eq. (19) can be expressed under steady state as follows:

$$Q_c = \overline{C}_\infty A\sqrt{S}\left(1 + T_{ph}K\right), \quad (28)$$

or

$$\overline{C}_\infty = Q_c / \left[A\sqrt{S}\left(1 + T_{ph}K\right)\right]. \quad (29)$$

Thus, if the equilibrium concentration $\overline{C}_\infty$ is set to the limit of precursor standard concentrations, then Q_c determined in eq. (28) denotes the emission limit of reducing substances under condition A. The emissions limit of reducing substances in the presence of chemical clearance power is always higher than the capacity determined by just physical clearance power (K=0), as the relationship $T_{ph}K = T_{ph} / T_{ch} \geq 0$ always holds true. In fact, $T_{ph}K$ can be referred to as a "characteristic process" of atmospheric oxidation as this relationship indicates the extent to which reducing substances can be oxidized within a reaction zone. Thus, as shown in eq. (29), when emission rate is given, the equilibrium concentration of a precursor decreases as long as $T_{ph}K$ increases. This means that the equilibrium concentration of precursors in small cities will be higher than that of larger ones under the same meteorology conditions. This is because there will be enough physical lifetime for precursors to oxidize in large cities. The quantitative change in product concentration after oxidation can therefore be expressed as the solution to eq. (17). This means that Q_c determined by eq. (28) is only related to the concentration of the precursor and is not related to oxidation product concentration. This relationship cannot therefore be used as the formula to calculate the atmospheric environmental capacity of precursors.

2.3 Changes in oxidation product concentration: A solution to kinetic eq. (17)

On the basis of eq. (20), a kinetic formula for the oxidation product (eq. (17)) can be expressed as follows:

$$\frac{\partial \overline{P}}{\partial t} = \frac{Q_p}{HS} - \frac{A}{H\sqrt{S}}\overline{P} + K\overline{C}_0 - K(\overline{C}_0 - \overline{C}_\infty)\left(1 - \mathrm{e}^{-\left(\frac{A}{H\sqrt{S}} + K\right)t}\right). \quad (30)$$

Thus, under equilibrium condition $\frac{\partial \overline{P}}{\partial t} = 0$, the solution $\overline{P}_\infty$, of eq. (30) is as follows:

$$\overline{P}_\infty = \frac{1}{A\sqrt{S}}\left(\frac{T_{ph}}{T_{ch} + T_{ph}}Q_c + Q_p\right). \quad (31)$$

In other words, as shown in eq. (31), when reaction rate, K is zero, $T_{ch} \to \infty$, and the equilibrium concentration of oxidation products depends on just their own primary emission rate, Q_p. In other situations, this depends on precursor emission. Thus, if the reaction zone is large enough and the physical self-purification power is small enough, then the characteristic physical retention time will be large enough. At the same time, when $T_{ph} \gg T_{ch}$, eq. (31) can be expressed as $\overline{P}_\infty \approx (Q_c + Q_p) / \mathrm{A}\sqrt{S}$ and the source, Q_c, of precursors remains an important concentration source for oxidation products.

Considering eq. (28), eq. (31) can be expressed as follows:

$$\overline{P}_\infty = KT_{ph}\overline{C}_\infty + \frac{Q_p}{\mathrm{A}\sqrt{S}}. \quad (32)$$

Thus, if Q_p is zero, it follows that:

$$\overline{P}_\infty / \overline{C}_\infty = \eta = KT_{ph} = T_{ph} / T_{ch}. \quad (33)$$

The ratio of product equilibrium concentration to the precursor, η, is equal to the characteristic process, KT_{ph}. Thus, as long as $K \neq 0$ and T_{ph} are large enough, the concentration of oxidation products will reach a sufficiently high level. A high concentration of fine particle pollution will occur across a large contaminated area given long-term and large-scale air stagnation weather, at the same time, precursor concentrations will be significantly reduced, as described by eq. (29).

Physical self-purification and chemical conversion contributions to changes in oxidation product concentration can also be analyzed via eq. (33). We therefore took the logarithm of the second equation in eq. (33) and then differentiated this to obtain $\Delta\eta / \overline{\eta} = \Delta K / \overline{K} + \Delta T_{ph} / \overline{T}_{ph}$, in which $\Delta\eta$ represents the change amplitude of the ratio of product equilibrium concentration to the precursor, as well as other quantities, are all similar in this regard. As noted by Cheng et al. (2008), the magnitude of simulation results, $\Delta K / \overline{K}$, within the Pearl River Delta is 10^0; this contrasts with the range of A values provided by eq. (22) as well as the literature (Xu et al., 2018) in which the magnitude of $\Delta T_{ph} / \overline{T}_{ph}$ was 10^1 or higher. This indicates that changes in the concentration of the oxidation product in the actual atmosphere are mainly due to the contribution of physical self-purification power of the atmosphere, while the value is more than one order of magnitude higher than the chemical conversion contribution.

According to eq. (31), the source intensity of the reducing

substances, the source intensity of the oxidation products, and the relationship of their equilibrium concentration can be combined to:

$$Q_c = \left(\overline{P}_\infty \mathrm{A}\sqrt{S} - Q_p\right)\left(\frac{1}{T_{ph}K} + 1\right), \tag{34}$$

when the products of the oxidation reaction are fine particles, then set $\overline{P}_\infty = P_s$, here P_s denotes the air quality standard limit for fine particles. If $Q_P < P_s A\sqrt{S}$, then the atmospheric environmental capacity, Q_c, of the precursors of secondary fine particles can be determined using eq. (34). At the same time, however, it is noteworthy that when $Q_P \geq \overline{P}_\infty A\sqrt{S}$, the concentration contributed by the primary emission rate of pollutant, P, will exceed the limit $\overline{P}_\infty$ and it remains impossible to consider the precursor.

Thus, under dynamic conditions, $\frac{\partial \overline{P}}{\partial t} \neq 0$, if we assume that the initial average concentration of secondary fine particle pollutants is $\overline{P} = \overline{P}_0$, then the solution to eq. (30) is as follows:

$$\overline{P} = \overline{P}_\infty + \left[(\overline{P}_0 - \overline{P}_\infty) - (\overline{C}_0 - \overline{C}_\infty)\left(1 - \mathrm{e}^{-\frac{t}{T_{ch}}}\right)\right]\mathrm{e}^{-\frac{t}{T_{ph}}}, \tag{35}$$

eq. (35) reveals the dependence of temporal variation of the concentration of fine particles with regard to precursor concentration as well as physical and chemical lifetimes.

2.4 The relationship between concentration ratio of oxidation products to precursor and the scale of the reaction zone

On the basis of solutions to kinetic eqs. (16) and (17) that describe concentration changes in the precursor and oxidation products, four concentrations and their relationship with atmospheric self-purification capacity can be derived. The equilibrium concentrations of reducing substances and oxidation products can be determined via eqs. (29) and (32), while the dynamic concentrations of reducing substances and oxidation products are provided by eqs. (24) and (35). Thus, if K in eq. (29) is set to zero, the equilibrium concentration of reducing substances in the absence of oxidants can be defined as $\overline{C}_{ina}$. It therefore follows that:

$$\overline{C}_{ina} = Q_c / A\sqrt{S}. \tag{36}$$

It is clear that if $\overline{C}_{ina}$ is set to the standard concentration limit, eq. (36) is the basic formula for determining atmospheric capacity in the literature (Xu et al., 2018). According to the definition of eq. (36) and eq. (29) is therefore:

$$\overline{C}_\infty = \overline{C}_{ina} / \left(1 + T_{ph}K\right). \tag{37}$$

As the reverse reaction process is not considered, the characteristic process $T_{ph}K$ is always greater than zero, and so $\overline{C}_\infty \leq \overline{C}_{ina}$ is true. Furthermore, when the atmospheric self-purification capacity, A, is given, the area covered by the pollutant reaction tends to zero. According to eq. (21), $T_{ph} \to 0$, and $\overline{C}_\infty \to \overline{C}_{ina}$, small area pollution is characterized by a high concentration of primary pollutants. In cases where there are no chemical reactions, $\overline{C}_\infty = \overline{C}_{ina}$ also holds true.

Thus, when the primary emission rate of oxidation products is set to $Q_p = 0$, the equilibrium concentration of the oxidation product in eq. (31) can be expressed as:

$$\overline{P}_\infty = \overline{C}_{ina} / \left[1 + \left(T_{ph}K\right)^{-1}\right], \tag{38}$$

eq. (38) indicates that $\overline{P}_\infty \leq \overline{C}_{ina}$ always holds true; thus, when the atmospheric self-purification capacity A is given, a larger area will be covered by the pollutant reaction and the larger the value of T_{ph}, then $\overline{P}_\infty \to \overline{C}_{ina}$. This indicates that a large pollution area can be easily characterized by high concentrations of oxidation products. In addition, when the chemical reaction rate $K \to \infty$, then $\overline{P}_\infty \to \overline{C}_{ina}$; this means that when $K \to 0$, then $\overline{P}_\infty \to 0$.

Adding eq. (37) to eq. (38), it follows that:

$$\overline{P}_\infty + \overline{C}_\infty = \overline{C}_{ina}. \tag{39}$$

This relationship shows that the inactive equilibrium molar concentration, $\overline{C}_{ina}$, is the sum of the equilibrium molar concentrations of the reducing substances and oxidation products, the upper limit of respective ranges. At a given atmospheric self-purification capacity and chemical reaction rate, responses to changes in reaction area will be reversed. In cases where a covered area is small, the concentration of precursors will be higher than that of oxidation products. In contrast, when a covered area is very large, the concentration of oxidation products will also be much larger than that of precursors. Eqs. (37) and (38) express this seesaw effect.

One intuitive explanation for this relationship assumes that the atmospheric mean self-purification power A at the normal value of 4×10^4 km^2 yr^{-1}, starts the weather A=0.7×10^4 km^2 yr^{-1}, which is an unfavorable for diffusion with a return period of about 30 days. The weather lasted for five T_{ph} periods and was followed by strong winds corresponding to A=30×10^4 km^2 yr^{-1} which also lasted for five T_{ph} periods. Initial concentration was therefore set to $\overline{C}_0$=100 μmol m^{-3}, $\overline{P}_0 = 0$. The covered areas of pollutants in this reaction were therefore 10^2 km^2 (small and medium-sized cities), 10^4 km^2 (large cities), 10^5 km^2 (provincial administrative areas), and 10^6km^2(inter-provincial urban agglomerations), respectively. In this case, the reaction rate K was 0.921×10^{-4} min^{-1} (average value in the daily variation chart), based on simulated data from the CBM-IV chemical mechanism outlined by Cheng et al. (2008). This mechanism considered 15 kinds of reducing substances and seven oxidation pathways,

including the heterogeneous oxidation of sulfur dioxide. On the basis of eqs. (20) and (18), a reaction rate $K=0.921\times10^{-4}$ min^{-1} was chosen to obtain a concentration curve of the active precursor $\overline{C}$. Thus, when K=0, a concentration curve $\overline{C}_{ina}$ of precursors in the absence of an oxidant can be obtained, while the P concentration curves of oxidation products can be obtained using eq. (35). These curves show time variation in average concentration in different zones with a time unit of 10^{-1} T_{ph}.

The data presented in Figure 1a–1d sequentially depict concentration trends within a weather change cycle from small cities to inter-provincial urban agglomerations. These data show that at the same initial concentration of reducing pollutants, the responses of differently-sized reaction zone areas to bad weather will be different. In the case of small cities, the concentration of precursors increases rapidly (Figure 1a), while for urban agglomerations or inter-provincial regions, the concentration of oxidation products suddenly increases (Figure 1d). The upper limits of these mark the equilibrium concentrations of pollutants in the absence of chemical activity. It is therefore both reasonable and meaningful to determine atmospheric environmental capacity via the limit of $\overline{C}_{ina}$ and eq. (36) (Xu et al., 2018). It is also the case that responses of pollution zones are different as a result of variation in the scale and residence time of the atmospheric system that enables low physical self-purification capacity. The slow-moving small-scale airflow stagnation region will lead to the increase in the concentration of precursors in the polluted zone within a small region, but when a large-scale airflow stagnation zone moves to a large-area polluted zone, the concentration of secondary pollutants increase dramatically. Indeed when a large-scale airflow stagnation system is blocked in a region where emission sources are concentrated, this can lead to large-area and high-concentration meteorological disasters involving secondary pollutants.

According to eqs. (33) and (21), it is also the case that:

$$\frac{\overline{P}_{\infty}}{\overline{C}_{\infty}}=\frac{KH\sqrt{S}}{A}, \tag{40}$$

eq. (40) describes the relationship between the concentration ratio of oxidation products to precursors, atmospheric self-purification capacity, and the area of a reaction zone at equilibrium state. This relationship means that the area range of emission zones can be set according to the range of atmospheric self-purification capacity and the reaction efficiency $\overline{P}_{\infty}/\overline{C}_{\infty}$, as follows:

$$S=\left(\frac{A}{KH}\frac{\overline{P}_{\infty}}{\overline{C}_{\infty}}\right)^2. \tag{41}$$

3. The atmospheric environmental capacity of secondary fine particle precursors across mainland China

3.1 Calculation formulae and parameters

Inactive atmospheric pollutants are controlled by only their

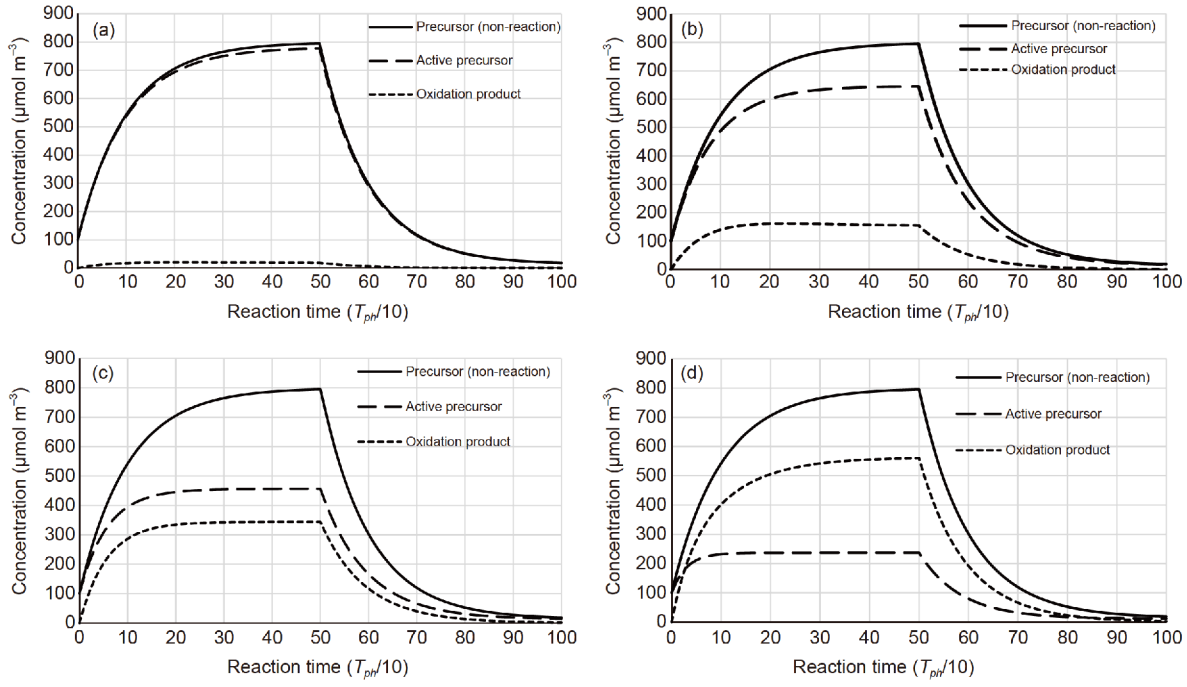

Figure 1 Concentrations of non-reacted and active precursors as well as oxidation products within different scale polluted zones under the same weather processes. (a) Reaction area is 100 square kilometers; (b) reaction area is 10000 square kilometers; (c) reaction area is 100000 square kilometers; (d) reaction area is million square kilometers.

own concentration standard limits and so their atmospheric environmental capacity can be calculated using eq. (28) when K=0. This is the equation for calculating capacity proposed by Xu et al. (2018). This relationship, eq. (34), can be applied to control secondary fine particle concentration, P, and in order to limit the emission rate of the precursor C, we assume $Q_p = 0$, $\overline{P}_\infty = P_s$ without loss of generality. Thus, P_s is the concentration limit of secondary particles, as follows:

$$Q_c = P_s A\sqrt{S}\left(\frac{1}{T_{ph}K}+1\right). \tag{42}$$

This equation was obtained under the integration assumptions inherent to eqs. (16) and (17). Thus, if area S is further divided into N sub-regions, i=1,⋯,N, the atmospheric self-purification index in each sub-region S_i is A_i. Previous work by Xu et al. (2018) and by the State Environmental Protection Administration (1991) suggests that the capacity Q_{ci} in the sub-region S_i can be defined as the value that obtained after weighting the total capacity Q_c by $A_i S_i / AS$ in S. It therefore follows that eq. (42) can be written as:

$$Q_{c,i} = P_s \frac{A_i S_i}{\sqrt{S}}\left(\frac{1}{T_{ph,i}K_i}+1\right). \tag{43}$$

In this expression, K_i and $T_{ph,i}$ denote respectively the oxidation rate and physical lifetime of the precursor in sub-region i, which are used to replace K and T_{ph}, and the latter can be calculated using formula (21).

This variable, $T_{ph,i}$, is determined by the local atmospheric self-purification index A_i, and the area of the reaction zone. The impact of reaction zone area on the formation rate of secondary product is significant. When the area of the reaction zone is given, it should first be considered that the activity frequency of the mesoscale air pressure system is the highest in daily weather process, and the characteristic value of the Rossby number of the system is $R_O \approx 10^0$, and corresponding area will be between 10^4 and 10^5 km^2, following Yang et al. (1991). Secondly, considering the fact that the spatial autocorrelation scale of fine particle concentrations in the atmosphere across mainland China is greater than 100 km (Mei et al., 2018), and that the effective area of a provincial administrative region, it is taken as 10^5 km^2. In addition, the overall area, S, is set to be the national land area of 960×10^4 km^2, while the area of a sub-region is the area represented by each of the 378 meteorological stations. The calculation method of the atmospheric self-purification index and the selection of parameters used here are the same previously noted (Xu et al., 2018). In terms of reaction rate, relatively systematic data is available in the Chinese literature including that obtained by Cheng et al. (2008) via Pearl River Delta simulation utilizing the CBM-IV chemical mechanism. Similarly, the concentration of hydroxyl [OH] measured at low altitude in North China by Ma et al. (2012) have been reported as well as the simulated data of reaction rate of NO_2 (or SO_2) and OH by Li et al. (2017). The former two are local data, while the latter is continent-wide data with four seasons. Considering that data from the Pearl River Delta conform to a more comprehensive oxidation reaction approach, the spatiotemporal distribution of data from Li Y et al. is relatively complete, and there is no significant difference compared with the results of Ma et al. (2012) across North China. We therefore reconstructed the spatiotemporal distribution of the pseudo-first order overall reaction rate for atmospheric oxidation in the continental region using the spatiotemporal weight of data from Li et al. (2017) as well as data for the Pearl River Delta as a mean. The reconstruction formula used here is as follows:

$$K_i = k_i \times K / \frac{1}{N}\sum_1^N k_i.$$

In this expression, K denotes average data from the Pearl River Delta, 0.921×10^{-4} min^{-1}. It is noteworthy, however, that k_i depends on the administrative area where a weather station is located and has been calculated previously according to the reaction rates of NO_2 (or SO_2) and OH (Li et al., 2017). Deducing on the basis of eq. (33), the ratio η of the equilibrium concentration of the product to the precursor is relatively tolerant of reaction rate errors and so reconstructed data will not cause serious differences in results. The standard reference value for the concentration of secondary fine particle is taken as p_s=p_r=100 (μmol m^{-3}). Thus, since K is used as the overall reaction rate of precursor in the calculation, the so-called capacity obtained via eq. (43) should be actually referred to as 'Lumped Capacity'.

3.2 The atmospheric environmental capacity of the lumped precursors, SO_2, NO_x, and NH_3 across mainland China

According to eq. (43) and other parameters, the climate averaged annual clearance quantity of lumped precursors across various regions of China was calculated. In addition, the Pearson-III curve was used to fit the A value, and the clearance quantity in the recurrence period was given and the results are summarized in Table 1. The fitting method was the same as that of Xu et al. (2016).

In order to calculate the mass concentration of a specific precursor, these were converted using eq. (44). This equation was deduced by equalizing the number of moles of reactants and products, as follows:

$$q_c = \frac{m_c}{m_p} \times Q_c \times r_p \times p_s / p_r. \tag{44}$$

In this expression, q_c is the capacity of precursor (annual clearance amount), 10^{10}g yr^{-1}, Q_c is the reference capacity of precursor, 10^{10} mol yr^{-1}, m_c is the relative molecular weight

Table 1 Annual reference clearance rate (10^{10}mol yr^{-1}) of precursors within the return period when the reference concentration of secondary particles in mainland China is set to 100 (μmol m^{-3})[a)]

Annual clearance amount/ return period (yr)	Average	5	10	20	30	100
Beijing	45.5	39.03	37.72	35.99	33.47	32.14
Tianjin	164.11	131.54	125.76	116.03	101.47	95.72
Hebei	580.33	498.18	482.87	456.85	416.74	400.35
Shanxi	1315.31	1105.6	1064.66	1011.08	933.62	893.28
Eastern Inner Mongolia	2440.93	2096.18	2054.88	1989.8	1875.38	1854.41
Western Inner Mongolia	1183.13	1023.64	1001.9	949.94	867.22	844.79
Liaoning	419.26	363.09	352.93	335.82	309.45	298.66
Jilin	667.5	570.85	552.59	523.13	478.01	458.56
Heilongjiang	1558.21	1253.94	1219.13	1169.29	1098.44	1068.99
Shanghai	11.5	9.83	9.52	9.19	8.74	8.46
Jiangsu	197.76	162.35	157.87	152.99	146.66	143.07
Zhejiang	247.71	212.65	211.09	201.58	186.48	186.09
Anhui	261.09	198.1	188.41	176.36	159.94	151.85
Fujian	253.83	193.49	182.66	170.19	153.3	143.86
Jiangxi	263.14	205.37	194.8	181.32	162.47	152.93
Shandong	267.62	227.87	222.27	209.22	188.45	182.57
Henan	182.55	151.7	145.69	138.03	127.09	121.3
Hubei	140.88	110.88	105.89	99.34	90.11	85.57
Hunan	258.07	208.57	199.49	188.59	173.49	165.19
Guangdong	671.32	590.94	575.2	556.07	528.75	513.17
Guangxi	504.69	427.21	411.93	393.4	367.17	352.37
Hainan	164.76	145.47	141.65	137.24	131.07	127.35
Sichuan	653.73	531.76	513.44	489.18	434.54	437.64
Chongqing	47.98	38.37	36.51	34.04	30.47	28.69
Guizhou	180.97	146.94	140.95	133.2	122.34	116.9
Yunnan	964.19	806.78	780.7	741.4	684.44	659.35
Tibet	5000.3	4054.82	3916.1	3750.52	3523.12	3400.85
Shaanxi	271.36	214.93	205.76	191	169.43	160.78
Gansu	1062.29	899.3	868.06	829.12	773.7	743.33
Qinghai	2077.28	1739.58	1682.48	1609.97	1507.89	1454.7
Ningxia	121.26	91.16	85.39	78.31	68.55	63.42
Xinjiang	2711.69	2195.56	2101.83	1971.4	1783.35	1694.55
Total	24890.3	20645.7	19970.1	19029.6	17635.4	17040.9

a) Eastern Inner Mongolia, The east-west boundary of the Inner Mongolia Autonomous Region is the watershed of the Yinshan Mountains.

of precursor, m_p is the relative molecular weight of oxidation products, r_p is the share of oxidation product in concentration of fine particle, p_s is the standard concentration of fine particles, μg m^{-3}, and p_r is the reference value of the concentration of secondary fine particle, 100 μmol m^{-3}. Thus, when $m_c / m_p = 1$ and the standard concentration limit of fine particles is 35 μg m^{-3}; on this basis, the climatic average q_t of the total capacity of all precursors across mainland China can be obtained according to Table 1:

$$q_t = Q_c \times p_s / p_r = 24890.3 \times 35 / 100$$
$$= 8711.605\ (10^{10}\ \text{g yr}^{-1}).$$

In order to control secondary fine particle pollution, the control parameters applied here include a concentration limit of 35 μg m^{-3}, where the ratio of sulfate (in terms of $(NH_4)_2SO_4$) is 0.30, and ratio of nitrate (in terms of $N_2H_4O_3$) is 0.20. In order to control ammonia capacity, $(NH_4)_2SO_4$, and $N_2H_4O_3$ were also set to 80% of the sum of sulfate and nitrate. The ratio of NO_2 to NO_x was set to 0.75 in order to control these oxides. These parameters and data are presented in Table 1 and so the atmospheric environmental capacity of SO_2, NO_x and NH_3 within each region were calculated.

In order to calculate the capacity of the precursor SO_2, r_p=0.30 was used, the ratio between the relative molecular

weight of SO_2 to $(NH_4)_2SO_4$ is m_c/m_p=0.48, the concentration limit p_s=35 μg m^{-3}, and the fine particle reference concentration p_r=100 μmol m^{-3}. Thus, on the basis of average annual data, Q_c=24890.3×10^{10} mol yr^{-1} as in Table 1, as follows:

$$q_c = 0.48 \times 24890.3 \times 0.30 \times 35 / 100$$
$$= 1254.5\ (10^{10}\ \text{g yr}^{-1}).$$

On the basis of the same calculation process, the capacities of SO_2 and NO_2 in each administrative region of mainland China were calculated, and the capacity of NO_x was converted from the latter. The corresponding capacity of NH_3 was then calculated using the molecular weight balance method for $(NH_4)_2SO_4$ and $N_2H_4O_3$ (Table 2).

It should be noted that capacity values for these precursors are closely related to the proportion of their oxides in fine

Table 2 Atmospheric environmental capacity of SO_2, NO_2 and NH_3 as fine particle precursors in mainland China with annual average and recurrence period of 10 years (10^{10} g yr^{-1})[a)]

Capacity	SO_2		NO_2		NO_x		NH_4	
	Annual average	10 years	Annual average	10 years	Annual average	10 years	Annual average	10 years
Beijing	2.3	1.9	1.8	1.5	2.5	2.0	1.52	1.42
Tianjin	8.3	6.4	6.6	5.0	8.9	6.8	5.49	4.72
Hebei	29.2	24.6	23.2	19.3	31.3	26.1	19.40	18.14
Shanxi	66.3	54.2	52.6	42.6	71.0	57.5	43.96	40.00
Eastern Inner Mongolia[a)]	123.0	104.6	97.6	82.2	131.8	111.0	81.58	77.20
Western Inner Mongolia	59.6	51.0	47.3	40.1	63.9	54.1	39.54	37.64
Liaoning	21.1	18.0	16.8	14.1	22.6	19.1	14.01	13.26
Jilin	33.6	28.1	26.7	22.1	36.0	29.8	22.31	20.76
Heilongjiang	78.5	62.1	62.3	48.8	84.1	65.8	52.08	45.80
Shanghai	0.6	0.5	0.5	0.4	0.6	0.5	0.38	0.36
Jiangsu	10.0	8.0	7.9	6.3	10.7	8.5	6.61	5.93
Zhejiang	12.5	10.7	9.9	8.4	13.4	11.4	8.28	7.93
Anhui	13.2	9.6	10.4	7.5	14.1	10.2	8.73	7.08
Fujian	12.8	9.3	10.2	7.3	13.7	9.9	8.48	6.86
Jiangxi	13.3	9.9	10.5	7.8	14.2	10.5	8.80	7.32
Shandong	13.5	11.3	10.7	8.9	14.5	12.0	8.94	8.35
Henan	9.2	7.4	7.3	5.8	9.9	7.9	6.10	5.47
Hubei	7.1	5.4	5.6	4.2	7.6	5.7	4.71	3.98
Hunan	13.0	10.2	10.3	8.0	13.9	10.8	8.63	7.49
Guangdong	33.8	29.3	26.9	23.0	36.3	31.1	22.44	21.61
Guangxi	25.4	21.0	20.2	16.5	27.3	22.2	16.87	15.48
Hainan	8.3	7.2	6.6	5.7	8.9	7.6	5.51	5.32
Sichuan	32.9	26.1	26.1	20.5	35.3	27.7	21.85	19.29
Chongqing	2.4	1.9	1.9	1.5	2.6	2.0	1.60	1.37
Guizhou	9.1	7.2	7.2	5.6	9.8	7.6	6.05	5.30
Yunnan	48.6	39.7	38.6	31.2	52.1	42.2	32.23	29.33
Tibet	252.0	199.3	200.0	156.6	270.0	211.5	167.13	147.12
Shaanxi	13.7	10.5	10.9	8.2	14.7	11.1	9.07	7.73
Gansu	53.5	44.2	42.5	34.7	57.4	46.9	35.51	32.61
Qinghai	104.7	85.6	83.1	67.3	112.2	90.9	69.43	63.21
Ningxia	6.1	4.3	4.9	3.4	6.5	4.6	4.05	3.21
Xinjiang	136.7	107.0	108.5	84.1	146.4	113.5	90.63	78.96
Total	1254.5	1016.6	995.6	798.8	1344.1	1078.4	831.91	750.22
Inactive	1302	1116	868	744	1085	930	521	447
Simulation	1363				1259		628	

a) The east-west boundary of the Inner Mongolia Autonomous Region is the watershed of the Yinshan Mountains. Inactive, Xu et al. (2018); Simulation, Xue et al. (2014).

particles. These proportions were based on data published in the literature, including in work by Deng et al. (2011), Cao et al. (2014), Jiang et al. (2017), Gu et al. (2016), Wei et al. (2017), Xing et al. (2016), Zhang et al. (2011), and Zhou et al. (2017). Control objectives must be determined according to the monitoring results of various regions and combined with the industrial structure for each administrative area in order to control the proportion of each oxide in fine particles.

The atmospheric environmental capacity of SO_2 and NO_x, as fine particle precursors listed in Table 2, are not significantly different from the atmospheric environmental capacity of inactive substances (Xu et al., 2018). The last column in Table 2 also lists the simulation results reported by Xue et al. (2014). Using time-of-day meteorological data for January, April, July, and October in 2010, they simulated the WRF-CAMx model, under the constraint of $PM_{2.5}$ less than or equal to 35 μmg m^{-3} in 333 prefecture-level cities across the Chinese mainland. After optimizing the reduction, the total atmospheric capacity of this region was obtained.

These results are basically consistent with the estimates in this paper. However, it should be noted that the premise is that order of reaction area is 10^5 km^2. Therefore, if a large stagnant weather system exceeding this scale stays in the reaction zone for a long time, perhaps due to the construction of urban agglomerations, this reaction area can be greatly increased. This means that atmospheric capacity density will decrease to some extent and will also lead to an increase in fine particle concentration.

The fine particle precursors listed in Table 2 are only oxides of sulfur and nitrogen. The other components in the secondary fine particles can be calculated in the same manner after clarifying the relationship between the precursor and the corresponding oxidation product.

3.3 The clearance density distribution of lumped precursors across mainland China

If formula (43) is divided by the *i*th partition area to define the precursor clearance density, that is, the clearance rate per unit area $Q_{c,d}$ is as follows:

$$Q_{c,d} = \frac{Q_{c,i}}{S_i} = P_s \frac{A_i}{\sqrt{S}} \left(\frac{1}{T_{ph,i} K_i} + 1 \right). \quad (45)$$

The data presented in Figure 2 shows the distribution of clearance rate density $Q_{c,d}$ in units of 10^6 mol yr^{-1} km^{-2}. Specifically, Figure 2a shows an climatological average value for the whole year, while Figure 2b shows the annualized climatic mean values in winter (November, December and January); Figure 2c is the annual average with a 10-year recurrence period, and Figure 2d shows the annualized average with a 10-year return period in winter (November, December, January).The quantity of precursors that can be removed per square kilometer per year in mainland China can be estimated on the basis of Figure 2 and eq. (46), as follows:

$$q_d = \frac{m_c}{m_p} \times Q_{c,d} \times r_p \times p_s / p_r . \quad (46)$$

As shown in Figure 2a, the average annual climate around Beijing is about $Q_{c,d}$=3.0×10^7 mol yr^{-1} km^{-2}; therefore according to eq. (46), the capacity of SO_2 per square kilometer in this region is therefore:

$$q_d = 3.0 \times 10^7 \times 0.48 \times 0.30 \times 35 / 100$$
$$= 1.51 \ (10^6 \text{ g a}^{-1} \text{km}^{-2}).$$

A planning area of 2×10^4 km^2 was established and therefore the capacity of SO_2 is 2×10^4×1.51×10^6=3.02 (10^{10} g yr^{-1}).

The data presented in Figure 2 reveal that the lumped atmospheric environmental capacity of fine particle precursors under the combined action of atmospheric physical and chemical clearance power and the distribution of clearance density of inactive pollutants reported by Xu et al. (2018) across mainland China are basically consistent. Some local differences are due to the uneven distribution of overall reaction rate among different regions. Low-value zones in Figure 2 are distributed in the southeast and northwest, while high-value zones are distributed in the Qinghai-Tibet Plateau, Inner Mongolia, and Northeast China.

3.4 Uncertainty analysis to determine precursor capacities

An uncertainty analysis is helpful for determining the confidence range of research results and providing a path to further increase certainty in estimations.

As the atmospheric capacity of precursors is determined according to eqs. (42)–(43), the decisive parameters can be divided into four components. That are: $A\sqrt{S}$ express the atmospheric three-dimensional flux, as shown in eq. (14); the physical lifetime T_{ph} of pollutants; the oxidation rate K; and the allocation of capacity among sub-regions.

Firstly, the three-dimensional flux comprises a two-dimensional horizontal component formed by airflow as well as vertical flux formed by one-dimensional dry and wet deposition. Horizontal flux depends on wind speed and boundary length of the polluted area, and so certainty is relatively high.

Vertical flux depends on dry and wet deposition rates, and so certainty is relatively low. At the scale of general cities or urban agglomerations, horizontal flux is more than an order of magnitude higher than vertical flux.

Secondly, T_{ph} refers to the characteristic time taken by pollutants to cross the boundary of a region. The main component of this characteristic time is proportional to the horizontal scale of the polluted zone, and inversely proportional to the advection-diffusion velocity, as shown in eqs.

(21)–(22). The characteristic time for fine particles to cross the horizontal direction plays a decisive role in physical life. According to the results of the City Air Pollution Prediction System (Xu et al., 2000) alongside the atmospheric self-purification capacity forecasting system (Zhu et al., 2018), certainty falls within a range between 60% and 80% or higher (characterized by the correlation coefficient of forecast effect). The order in which further research is required will therefore be to address the thickness of the mixed layer, the wash-out-ratio, and dry deposition velocity throughout the area.

Thirdly, in terms of oxidation rate, the atmospheric chemical kinetic equation is the principle used for specific reducing pollutants and corresponding oxidants. The concept 'lumped' was therefore used in this study to gain a quick capacity estimate. In a specific area, a definite atmospheric environmental precursor capacity can be calculated according to the monitoring data for local pollutant concentration, specific reducing pollutants, and corresponding oxidants that depend on industrial structure as well as the control components of secondary fine particles. The oxidation rate of some specific substances can be related to certain meteorological elements, such as humidity, temperature, and solar radiation intensity. This area will also require further research and analysis before quantitative results can be obtained. Analysis based on eq. (33) shows that change in physical self-purification capacity plays a major role in the concentration of secondary fine particles. Indeed, with the exception of special cases, uncertainty caused by general oxidation rate turns out to not be most important.

Finally, the distribution of capacity among sub-regions is essentially a problem of pollutant transport. In the case of a single large polluted area with no emissions around, capacity is determined according to formula (42) and therefore certainty is relatively high. Thus, if there are N sub-regions within this region, transmission parameters between regions belong to the internal parameters of the large area and can be processed via the weighted allocation method. Weight can be expressed via a sub-region interaction matrix (i.e., a transmission weighting factor tensor) constructed on the basis of physical self-purification factors such as wind direction, speed, and stability, as well as precipitation at each time in each sub-region. This method is similar to the multi-source simulation and can, however, only be performed for limited scenarios. Because of the limited number of samples in this scenario, result certainty is limited, and it remains difficult to obtain characteristic parameters for the climate statistics that describe the capacity of each sub-region.

The weighting function, $A_i S_i / AS$, defined by State Environmental Protection Administration (1991) is a first-order

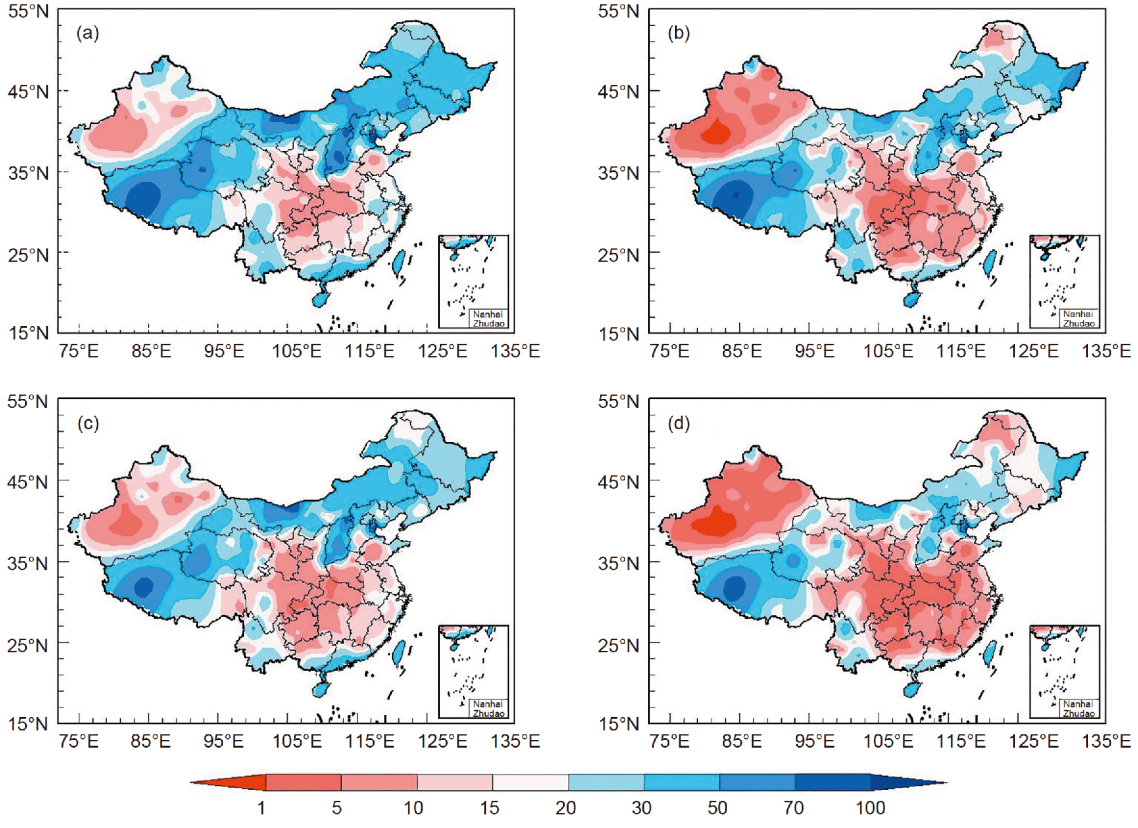

Figure 2 Map to show the distribution of clearance density, $Q_{c,d}$, for fine particle precursors across mainland China (10^6 mol yr^{-1} km^{-2}). (a) Average value for the whole year; (b) annualized average value for the winter; (c) ten year annual average value; (d) ten year annualized average value in winter. Annualized average clearance rate in winter is the average clearance rate in winter×4.

approximation of the transmission weighting factor. The weighted weather factor in this case is the self-purification index, because heavy pollution with a weak physical self-purification capacity will occur in low-index weather conditions with static-small wind and a thin boundary layer; this result is of great importance for determining the probability distribution of atmospheric environmental capacity. In this kind of weather, the long-distance transportation of pollutants is generally less than local accumulation in an active region. It is therefore convenient to calculate a climatologically characteristic statistic for the "lumped" capacity of the precursors for each sub-region based on this weighting factor. This can also be corrected via simulation based on this lumped capacity to obtain a higher order approximation of the capacity distribution.

The method proposed on the basis of eq. (43) to obtain the atmospheric capacity of secondary fine particle precursors avoids some of the uncertainty caused by the use of a source list, the selection of monitoring points, and the formulation of an optimized reduction plan. Meteorological parameters expressed by the self-purification index in a probability form of increase the certainty of meteorological condition selection.

4. Conclusions

According to the solution of the atmospheric chemical kinetic equation constructed in this paper, and the statistical results of physical self-purification, and the spatiotemporal distribution of the atmospheric overall oxidation reaction rate, the reference atmospheric capacity of all precursors in the Chinese mainland was 24890.3×10^{10} mol yr^{-1}, when fine particles ($PM_{2.5}$) reaches the annual reference concentration of 100 μmol m^{-3}. Thus, when the ratio of sulfate and nitrate in fine particles are set to 0.3 and 0.2, respectively, and the standard limit of fine particles is 35 μg m^{-3}, the average annual climatic capacity of SO_2, NO_x and NH_3 are estimated to be 1254.5, 1344.1, and 831.9 (10^{10}g yr^{-1}), respectively.

The clearance density of precursors in Tibet, Qinghai, Inner Mongolia to the Northeast China are highest across mainland China, while low values are seen in Xinjiang, Sichuan and Guizhou provinces, southern parts of Gansu and Shaanxi provinces, and in each province in Southeast China. The overall situation is generally similar to the distribution of inactive pollutant clearance densities reported by Xu et al. (2018).

The concentration ratio of secondary pollutants versus their precursors in a polluted region is equal to the ratio between the chemical and physical lifetime of the precursor.

Secondary pollution is generally serious, and the concentration of the precursor is low, if the contaminated area is wide, the scale of air stagnation is large, and stagnation time is long. However, when the polluted area is small, the precursor concentration is high and the secondary pollutant concentration is low. This means that high concentrations of secondary pollutants occur easily within large-scale urban agglomerations, while pollution caused by high concentrations of precursors occurs easily within isolated small cities.

The sum of the molar equilibrium concentrations of precursors and reaction products will not exceed the molar equilibrium concentration obtained by using the precursor as an inactive material.

The atmospheric environmental capacity of a precursor depends on the length of its physical and chemical lifetimes as well as their ratio. In order to reasonably and accurately determine atmospheric environmental capacity, it is therefore important to further study, analyze, and count the physical and chemical lifetime of precursors in various regions based on actual meteorological observations and monitor the results of pollutant concentrations in an open atmospheric environment.

The atmospheric chemical kinetic equation established in this study, theoretically can also be used to describe the reaction process of lumped or specific reducing pollutants and associated oxidants. The equations derived here, especially eqs. (25)–(27), can therefore theoretically be used to deduce the rate of an oxidation reaction of reducing pollutants in the atmosphere on the basis of meteorological and concentration data from fixed ambient air quality monitoring points.

Acknowledgements *Thanks to the reviewers for their valuable constructive comments during the review. This study was supported by S & T Development Program (Grant No. CAMS 2018KJ026).*

References

Alkezweeny A J, Powell D C. 1977. Estimation of transformation rate of SO_2 to SO_4 from atmospheric concentration data. Atmos Environ, 11: 179–182

Byun D, Schere K L. 2006. Review of the governing equations, computational algorithms, and other components of the Models-3 community multiscale air quality (CMAQ) modeling system. Appl Mech Rev, 59: 51–77

Cao L X, Geng H, Yao C T, Zhao L, Duan P L, Xuan Y Y, Li H. 2014. Characteristics of chemical constituents of fine particulate matter during haze episode in Taiyuan City (in Chinese). China Environ Sci, 34: 837–843

Cheng Y L, Wang X S, Liu Z R, Bai Y H, Li J L. 2008. A new method for quantitatively characterizing atmospheric oxidation capacity. Sci China Ser B-Chem, 51: 1102–1109

Cooper J A, Watson Jr J G. 1980. Receptor oriented methods of air particulate source apportionment. J Air Pollut Control Assoc, 30: 1116–1125

Deng L Q, Li H, Chai F H, Lun X X, Chen Y Z, Wang F W, Ni R X. 2011. The pollution characteristics of the atmospheric fine particles and related gaseous pollutants in the northeastern urban area of Beijing (in Chinese). China Environ Sci, 31: 1064–1070

Grell G A, Peckham S E, Schmitz R, McKeen S A, Frost G, Skamarock W C, Eder B. 2005. Fully coupled "online" chemistry within the WRF model. Atmos Environ, 39: 6957–6975

Jiang L, Zhu B, Wang H L, Sha D D, Shi S S. 2017. Characteristics of water-soluble ions in the haze and mist days in winter in Yangtze River Delta (in Chinese). China Environ Sci, 37: 3601–3610
Li Y, Tang W, Ding F, He Y J, Zhu X Y, Meng F. 2017. Study on a method for calculating conversion coefficient of secondary sulfate and nitrate in atmosphere (in Chinese). Environ Pollut Control, 39: 1348–1352
Lin Y, Ye Z X, Yang H J, Zhang J, Zhu Y M. 2017. Pollution level and source apportionment of atmospheric particles PM_1 in downtown area of Chengdu (in Chinese). China Environ Sci, 37: 3220–3226
Ma J Z, Wang W, Chen Y, Liu H J, Yan P, Ding G A, Wang M L, Sun J, Lelieveld J. 2012. The IPAC-NC field campaign: A pollution and oxidization pool in the lower atmosphere over Huabei, China. Atmos Chem Phys, 12: 3883–3908
Mei Y, Zhang W T, Yang Y, Zhao Y, Li L L. 2018. Uncertainty assessment of $PM_{2.5}$ probability mapping by using spatio-temporal indicator kriging (in Chinese). China Environ Sci, 38: 35–43
Paatero P, Tapper U. 1993. Analysis of different modes of factor analysis as least squares fit problems. Chemo Intell Lab Syst, 18: 183–194
Pasquill F, Smith F B.1983. Atmosperic Diffusion. 3rd ed. New York: Ellis Horwood Limited. 383
Gu F T, Hu M, Wang W, Li M R, Guo Q F, Wu Z J. 2016. Characteristics of $PM_{2.5}$ pollution winter and spring of Beijing during 2009–2010 (in Chinese). China Environ Sci, 36: 2578–2584
State Environmental Protection Administration. 1991. Handbook of Total Methods for Controlling Urban Air Pollution (in Chinese). Beijing: China Science Press. 164–170
Seinfeld J H, Pandis S N. 2016. Atmospheric Chemistry and Physics: From Air Pollution to Climate Chang. New Jersey: John Wiley & Sons
Tang X Y, Zhang Y H, Shao M. 2006. Atmospheric Environmental Chemistry (in Chinese). 2nd ed. Beijing: Higher Education Press. 125–210
Wei F F, Liu W, Lu X B, Wang Q G, Ge Y, Hao J. 2017. Temporal and spatial characteristics of $PM_{2.5}$ in Nanjing (in Chinese). China Environ Sci, 37: 2866–2876
Xing J P, Shao L Y, Li H, Guo W, Wang W H, Zuo X C. 2016. ATR-FTIR characteristics of organic functional groups and inorganic ions of the haze $PM_{2.5}$ in Beijing (in Chinese). China Environ Sci, 36: 1654–1659
Xu D H, Zhu R. 2000. Atmospheric advective and dispersion nonstatic box-model for prediction of the potential index of airborne pollutant. Quart J Appl Meteorol, 11: 1–12
Xu D H, Wang Y. 2013. Plume footprints analysis for determining the bearing capacity of atmospheric environment (in Chinese). Acta Scientiae Circumstantiae, 33: 1734–1740
Xu D H, Wang Y, Zhu R. 2016. The atmospheric environmental capacity coefficient cumulative frequency curve fitting and its application (in Chinese). China Environ Sci, 36: 2913–2922
Xu D H, Wang Y, Zhu R. 2018. Atmospheric environmental capacity and urban atmospheric load in mainland China. Sci China Earth Sci, 61: 33–46
Xu H, Xiao Z M, Kong J, Yuan J, Li P, Guan Y C, Deng X W, Zhang Y F, Han S Q. 2017. Characteristic of atmospheric heavy pollution episodes in Winter of Tianjin (in Chinese). China Environ Sci, 37: 1239–1246
Xue W B, Fu F, Wang J N, He K B, Lei Y, Yang J T, Wang S X, Han B P. 2014. Modeling study on atmospheric environment capacity of major pollutants constrained by $PM_{2.5}$ compliance of Chinese cities (in Chinese). China Environ Sci, 34: 2490–2496
Yang G X, He Q Q, Lu H C. 1991. Meso-Meteorology (in Chinese). Beijing: China Meteorological Press. 2–4
Zhu R, Zhang C J, Mei M. 2018. Climate characteristics and application of atmospheric self-purification capacity index (in Chinese). China Environ Sci, 38: 3601–3610
Zhang Y H, Duan Y S, Gao S, Wei H P, Sha F, Cai Y, Shen L P. 2011. Characteristics of fine particulate matter during a typical air pollution episode in Shanghai urban area (in Chinese). China Environ Sci, 31: 1115–1121
China National Standard GB/T34299-2017. 2018. Grades of Atmospheric Self-Purification Capability (in Chinese). Beijing: Standard Press
Zhou T, Yan C Q, Li X W, Cai J, Guo X S, Wang R, Wu Y S, Zeng L M, Zhu W, Zhang Y H, Zheng M. 2017. Chemical characteristics and sources of $PM_{2.5}$ in urban and rural sites in the North China Plain during summer (in Chinese). China Environ Sci, 37: 3227–3236

(Responsible editor: Qiang ZHANG)